EUROPHYSICS LETTERS 15 August 2004

Europhys. Lett., **67** (4), pp. 655–661 (2004)
DOI: 10.1209/epl/i2004-10093-9

Peak effect and surface crystal-glass transition for surface-pinned vortex array

B. Plaçais[1], N. Lütke-Entrup[1], J. Bellessa[1], P. Mathieu[1], Y. Simon[1] and E. B. Sonin[2]

[1] *Laboratoire Pierre Aigrain, Département de Physique de l'Ecole Normale Supérieure 24 rue Lhomond, 75005 Paris, France*
[2] *Racah Institute of Physics, Hebrew University of Jerusalem - Jerusalem 91904, Israel*

(received 5 March 2004; accepted in final form 7 June 2004)

PACS. 74.25.Qt – Vortex lattices, flux pinning, flux creep.
PACS. 64.60.Cn – Order-isorder transformations; statistical mechanics of model systems.

Abstract. – We present a theoretical and experimental study of the peak effect in the surface pinning of vortices. It is associated with a sharp transition in the vortex slippage length which we relate to a crossover from a weakly disordered crystal to a surface glass state. Experiments are performed on ion-beam–etched Nb crystals. The slippage length is deduced from 1 kHz–1 MHz linear AC penetration depth measurements.

A peak in the *critical current vs. magnetic field* plot, the peak effect (PE), is observed in superconductors close to the transition line where the critical current vanishes. From the very first studies [1–4] it was supposed that PE originates from softening of the vortex lattice (VL) by disorder near the transition. This results in a more effective vortex pinning, which corresponds to a higher critical current. The phenomenon is directly connected with a fundamental problem of condensed-matter physics: the competition between elasticity and disorder. Numerous scenarios of PE have been discussed, but all of them dealt with the competition between vortex elasticity and *bulk* pinning. Here we present an essentially different scenario of PE: it is *surface* pinning of vortices which interplays with *bulk* vortex elasticity.

A controlled surface roughness $\zeta(\boldsymbol{r})$ is obtained by etching the Nb sample surfaces with 500 eV Ar^+ ions (fig. 1). The sputtering of Nb atoms by low-energy ions is a stochastic process. It gives rise to a white corrugation spectrum $S_\zeta(\boldsymbol{k}) = \int \mathbf{d}r\, e^{-i\boldsymbol{k}\boldsymbol{r}} \langle \zeta(\boldsymbol{r}+\boldsymbol{R})\zeta(\boldsymbol{R})\rangle_{\boldsymbol{R}} \simeq a^3\overline{\Delta z}/\pi$ for $|\boldsymbol{k}| < 1/a$, where $a = 0.26$ nm is the Nb lattice parameter and $\overline{\Delta z}$ the average sputtering depth. In our experiment $\overline{\Delta z} \sim 10\,\mu$m for a 90 min exposure to a 1.5 mA/cm^2 Ar^+ flux so that $S_\zeta \sim 50\,\mathrm{nm}^4$ and the total roughness $\zeta^* = \sqrt{\langle \zeta(\boldsymbol{r})^2\rangle} < (a\overline{\Delta z})^{1/2} = 50$ nm. Atomic force microscopy (AFM) in fig. 2 confirms the above estimates with $S_\zeta(k) \simeq 40\,\mathrm{nm}^4$ for $k \lesssim 40\,\mu\mathrm{m}^{-1}$. Unfortunately, the finite AFM-tip radius masks the large k spectrum, so that we can only bracket the upper cut-off k_c of $S_\zeta(k)$ in the range $10^{-2} < k_\mathrm{c}a < 1$. This entails a large uncertainty in $\zeta^* = 0.5$–50 nm. Importantly for our scenario, AFM data indicate the presence of roughness at small scale, with wave numbers $k \sim a_0^{-1} \simeq (50\,\mathrm{nm})^{-1}$, where $a_0 = \sqrt{\pi B/\varphi_0}$ is the VL reciprocal unit and $\varphi_0 = h/2e$ is the flux quantum. Note that a roughness is smaller than vortex spacing so that the weak surface pinning approximation used below is justified.

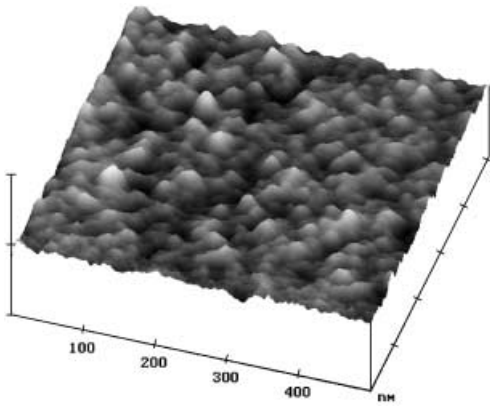

Fig. 1

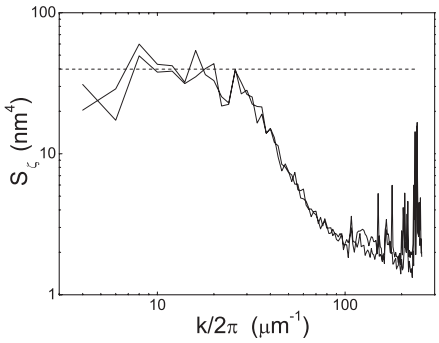

Fig. 2

Fig. 1 – Atomic-force microscopy (AFM) picture of the etched Nb surface. The vertical scale is 10 nm per division.

Fig. 2 – Spectrum of the surface corrugation. The dashed line is a guide. The cut-off at $\sim 40\,\mu\mathrm{m}^{-1}$ is due to AFM tip diameter.

The peak effect is generally observed in the critical current data $I_\mathrm{c}(B)$ or $I_\mathrm{c}(T)$. We see it in our samples as well, but since $I_\mathrm{c} \gtrsim 20\,\mathrm{A}$ are quite large, we prefer to rely on the AC linear surface impedance $Z(\omega) = -i\omega\mu_0\lambda_\mathrm{AC}$ which is a more accurate and non-destructive probe of the vortex state, especially in the vicinity of a transition. According to [5,6], the AC penetration depth λ_AC in thick samples is given by

$$\frac{1}{\lambda_\mathrm{AC}} = \frac{1}{L_\mathrm{S}} + \left[\frac{1}{\lambda_\mathrm{C}^2} + i\omega\mu_0\sigma_\mathrm{f}\right]^{1/2}, \quad L_\mathrm{S} = \frac{l_\mathrm{S}B}{\mu_0\varepsilon}\,. \tag{1}$$

Here σ_f is the flux-flow resistivity, $\varepsilon\varphi_0$ is the vortex-line tension, and λ_C the Campbell depth for bulk pinning [7]. Expression (1) deviates from the Coffey-Clem theory [8] by the addition of a surface pinning term $1/L_\mathrm{S}$. The surface pinning length $L_\mathrm{S} \sim 0.1$–$100\,\mu$m can indeed simulate a Campbell length at low frequency but gives a very different behaviour at finite frequency [5, 6]. The above expression was derived within the frame of the *two-mode electrodynamics* [5,9], which incorporates the surface pinning by introducing a phenomenological boundary condition,

$$\varepsilon\varphi_0\left[\frac{\boldsymbol{u}}{l_\mathrm{S}} + \frac{\partial\boldsymbol{u}}{\partial z}\right] = 0, \tag{2}$$

imposed on the VL displacement $\boldsymbol{u}(z)$ at the surface of the sample, which occupies the semi-space $z < 0$. Here l_S is a *slippage length* and the displacement $\boldsymbol{u}$ is averaged over the position vectors $\boldsymbol{r}$ in the xy plane. Equation (2) represents the balance between the pinning force $-\varepsilon\varphi_0\boldsymbol{u}/l_\mathrm{S}$ and the line tension force $\varepsilon\varphi_0\partial\boldsymbol{u}/\partial z$. In the DC experiment the critical current is proportional to ε/l_S (see ref. [6], p. 80). If the magnetic field B is close to an upper critical field B_c2, when the peak effect takes place, the critical current is proportional to $1/L_\mathrm{S}$. Thus the peak of $1/L_\mathrm{S}$ as a function of B is relevant for the peak effect in both DC and the AC measurements.

If vortices do not interact, the slippage length l_S does not depend on vortex density and is on the order of a curvature radius of the surface profile (individual pinning). But, in general,

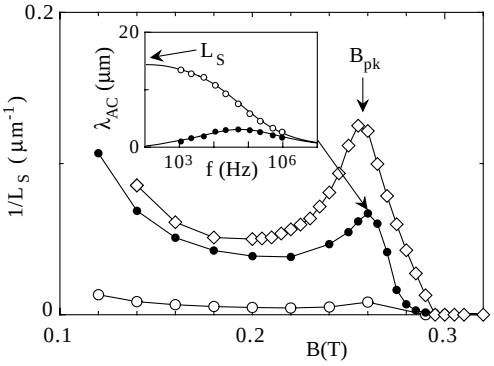

Fig. 3

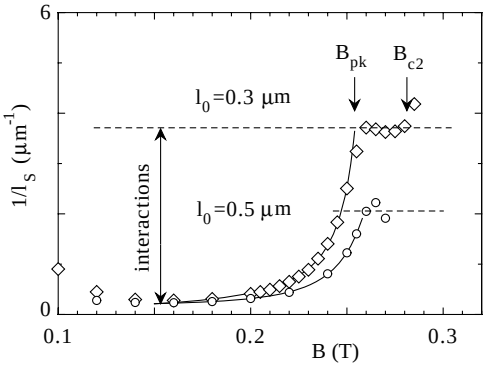

Fig. 4

Fig. 3 – Peak effect in the elastic response $L_{\rm S}^{-1}(B)$ of a surface-pinned vortex array at $T = 4.2\,{\rm K}$. Diamonds and full circles correspond to the 45 degree and perpendicular field orientations. Empty circles are the pristine sample measurement. Inset: the frequency dependence of the real and imaginary parts (open and full circles, respectively) of the penetration depth $\lambda_{\rm AC}(B, f)$ from which $L_{\rm S}$ is deduced. Solid lines are theoretical fit to eq. (1) with $\lambda_{\rm C} = \infty$, $\sigma_{\rm f}^{-1} = 10\,{\rm n}\Omega\,{\rm cm}$ and $L_{\rm S} = 14.9\,\mu{\rm m}$.

Fig. 4 – The slippage length $l_{\rm S}(B)$ for a vortex array at a rough surface. It is deduced from the $L_{\rm S}$ data according to $l_{\rm S} = L_{\rm S}\mu_0\varepsilon/B$ in eq. (1). The effect of vortex interactions in the collective-pinning regime below $B_{\rm pk}$ is visible as a suppression of $1/l_{\rm S}(B)$. Solid lines are power law fits.

$l_{\rm S}$ may depend on vortex density, *i.e.* on magnetic field (see fig. 4). If vortices strongly interact the theory of collective pinning [4] assumes that within the so-called Larkin-Ovchinnikov domain of size $L_{\rm c}$ the vortices move mostly coherently without essential deformation of the vortex lattice. But then because of the random directions of pinning forces on every vortex, the total force on vortices in the domain is proportional to $\sqrt{N_{\rm c}}$ and not to $N_{\rm c} = L_{\rm c}^2/a_0^2$, the number of vortices in the domain. Correspondingly, the pinning force per vortex must be smaller by the factor $\sqrt{N_{\rm c}} = L_{\rm c}/a_0$, *i.e.* $1/l_{\rm S} = 1/l_0\sqrt{N_{\rm c}} = a_0/l_0 L_{\rm c}$. $L_{\rm c}$ is usually derived from the balance between the elastic and pinning energy. Pinning is collective as long as $N_{\rm c} \gg 1$. The condition $N_{\rm c} \sim 1$ (or $l_{\rm S} \sim l_0$) determines the crossover from the collective to the individual pinning. Later in the paper we shall derive $l_{\rm S}$ without these heuristic arguments.

Figure 3 shows the PE in the inverse surface-pinning length. The sample, with dimensions $25 \times 10.1 \times 0.87\,{\rm mm}^3$, was annealed in ultra-high vacuum which gives a low residual resistivity $\rho_{\rm n} = 11\,{\rm n}\Omega{\rm cm}$ (resistivity ratio ~ 1300) and an upper critical field $B_{\rm c2} = 0.29\,{\rm T}$ at $4.2\,{\rm K}$ [10]. Data points are obtained by fitting the penetration depth spectra (inset of fig. 3) with eq. (1). Metastability in the vortex density ($\pm 0.005\,{\rm T}$) and/or arrangement is removed by feeding a large transient current $I \gg I_{\rm c}$ in the sample prior to measurement. The abrupt onset of the AC-flux penetration along the samples edges which are parallel to the field precludes quantitative analysis for $B \gtrsim 0.95 B_{\rm c2}$; this difficulty is overcome by working in oblique field (diamonds in fig. 3). Already present in the pristine sample, the PE is strongly enhanced in ion-etched samples (circles in fig. 3). By contrast, chemically etched samples show little PE but a large increase of pinning at lower fields. We think that this difference is due to the lack of small-scale corrugation in the wet-etching techniques.

We quantitatively separate the bulk and surface pinning contributions, $\lambda_{\rm C}$ and $L_{\rm S}$, by fitting the full $1\,{\rm kHz}$–$1\,{\rm MHz}$ spectrum $\lambda_{\rm AC}(f)$ with eq. (1). Remarkably, we always find that $\lambda_{\rm C}$ is much larger than the sample thickness ($\sim 1\,{\rm mm}$), whereas $L_{\rm S} \sim 5$–$100\,\mu{\rm m}$, meaning

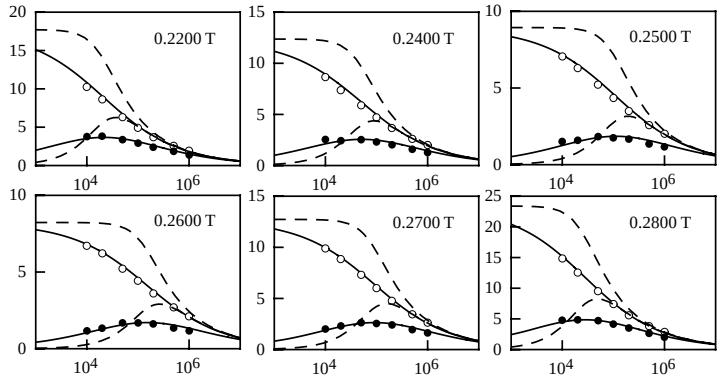

Fig. 5 – Typical spectra of the linear-response $\lambda_{\rm AC}(B, f)$ in tilted magnetic field. Upper and lower spectra correspond to magnetic fields, respectively, above and below the peak shown in fig. 3. Vertical units are in microns and frequencies are in Hz. Open and full circles correspond, respectively, to the real and imaginary parts. Solid lines are theoretical fits to eq. (1) with $\lambda_{\rm C} = \infty$, $\sigma_{\rm f}^{-1} = 5.4$, 6.2, 7, 8.2, 11.8, 12.36 nΩ cm and $L_{\rm S} = 17.7$, 12.4, 8.9, 8.2, 12.7, 23.4 μm. Dashed lines are theoretical lines for pure bulk pinning obtained by interverting values of $\lambda_{\rm C}$ and $L_{\rm S}$ keeping $\sigma_{\rm f}$ unchanged.

that bulk pinning is negligible. As seen in fig. 5, this observation is true for $\lambda_{\rm AC}(f)$ spectra taken on both sides of the peak; it confirms that surface pinning is most relevant in our experiment. The oblique-field (45 degree) data are larger by a factor ~ 2; this is due to surface reinforcement of superconductivity in tilted fields. Otherwise, data are similar at lower temperatures with however larger $B_{\rm pk} = 0.95 B_{\rm c2}$ (1.8 K) and a less pronounced peak sometimes resembling a shoulder.

Using the Abrikosov expression [11], $\mu_0 \varepsilon \simeq (B_{\rm c2} - B)/2.32\kappa^2$ with $\kappa = \lambda/\xi = 1.3$ (ξ is the coherence length and λ is the London penetration depth), we deduce from eq. (1) the $l_{\rm S}(B)$ data in fig. 4. The high-field plateaus $l_{\rm S}(B)$ above $B_{\rm pk}$ are suggestive of individual pinning, when $l_{\rm S} \sim l_0$ does not depend on B. Note that the value of the contact angle for VL at the surface, $a_0/l_0 \simeq 0.1$ estimated from $l_0 \simeq 0.5\,\mu$m (normal field) and $a_0 = 50$ nm, fits in the window $0.01 < \zeta^*/a_0 < 1$ prescribed by corrugation geometry. By contrast, the strong suppression of $1/l_{\rm S}$ below $B_{\rm pk}$ (factor ~ 10 in oblique field) reflects the *collective* regime of surface pinning, which was known earlier in rotating ^{3}He [12]. The transition is sharp unlike the continuous ones reported in refs. [13, 14]. Thus, the experiment provides an evidence that PE is accompanied by the crossover from collective to individual surface pinning. In the following, we give the theory for the slippage length $l_{\rm S}(B)$ in the collective regime and explain its vanishing at the PE transition.

The first step of our analysis addresses the response of the semi-infinite VL to a Fourier component $\boldsymbol{f}(\boldsymbol{r}) = \boldsymbol{f}(\boldsymbol{k}) e^{i\boldsymbol{k}\boldsymbol{r}}$ of the surface force on vortices. The force produces vortex displacements in the sample bulk ($z < 0$) in the form $\boldsymbol{u}(\boldsymbol{r}, z) = \sum_{k_z} \boldsymbol{U}(\boldsymbol{k}, k_z) e^{i\boldsymbol{k}\boldsymbol{r} + ik_z z}$. We look for the elastic constant $C(\boldsymbol{k}) = f(\boldsymbol{k})/u(\boldsymbol{k})$, connecting the Fourier components of the surface force $\boldsymbol{f}(\boldsymbol{k})$ to the surface displacement $\boldsymbol{u}(\boldsymbol{k}) = \sum_{k_z} \boldsymbol{U}(\boldsymbol{k}, k_z)$. The force is assumed to be transverse, $[\boldsymbol{f}(\boldsymbol{k}), \boldsymbol{U}(\boldsymbol{k}, k_z) \perp \boldsymbol{k}]$, since VL compressibility is quite low and the response to the longitudinal force is weak. The possible values of out-of-plane wave vector component k_z must be found from the equation of the elasticity theory:

$$\sum_{k_z} C_{66} k^2 + C_{44}(\boldsymbol{k}, k_z) k_z^2 \sum_{k_z} \boldsymbol{U}(\boldsymbol{k}, k_z) = 0, \tag{3}$$

where C_{66} is the shear modulus and

$$C_{44}(\boldsymbol{k}, k_z) = \frac{B^2}{\mu_0} \frac{1}{1 + \lambda^2(k^2 + k_z^2)} + \varepsilon B \tag{4}$$

is the tilt-modulus, which takes into account nonlocal effects due to long-range vortex-vortex interaction. The general solution of eq. (3) is a superposition of *two evanescent modes* in the bulk, $\boldsymbol{u}(\boldsymbol{r}, z) = e^{i\boldsymbol{k}\boldsymbol{r}}[\boldsymbol{U}(\boldsymbol{k}, p_1)e^{p_1 z} + \boldsymbol{U}(\boldsymbol{k}, p_2)e^{p_2 z}]$ with $p_1 \approx k\sqrt{C_{66}/\varepsilon B} \ll 1/\lambda$ and $p_2 \approx 1/\lambda\sqrt{B/\mu_0\varepsilon} \gg 1/\lambda$. In order to determine the two amplitudes $\boldsymbol{U}(\boldsymbol{k}, p_1)$ and $\boldsymbol{U}(\boldsymbol{k}, p_2)$, we need a second boundary conditions. It is imposed on the magnetic field, which is determined from the London equation, $\boldsymbol{h}(\boldsymbol{k}, k_z) = ik_z B\boldsymbol{U}(\boldsymbol{k}, k_z)[1 + \lambda^2(k^2 + k_z^2)]^{-1}$, and should vanish at the sample border (transverse waves). Eventually, this yields for $C_{66} \ll \varepsilon B \ll B^2/\mu_0$

$$C(k) \approx k\varphi_0 \sqrt{\frac{C_{66}}{\mu_0} \frac{(1 + \lambda^2 k^2 \mu_0 \varepsilon/B)}{1 + \lambda^2 k^2}}\,. \tag{5}$$

At large λk, eq. (5) gives $C(k) = k\varphi_0\sqrt{\varepsilon C_{66}/B}$.

The second step consists in calculating the deformations produced by surface pinning from the corrugation profile $\zeta(\boldsymbol{r})$. The random force on the vortices is $\boldsymbol{f}(\boldsymbol{r}_i) = -\varepsilon\varphi_0 \boldsymbol{\nabla}\zeta(\boldsymbol{r}_i)$, where $\boldsymbol{r}_i$ is the 2D position vector of the i-th vortex. The Fourier component of the force is $\boldsymbol{f}(\boldsymbol{k}) = -\varepsilon B \sum_{\boldsymbol{Q}} i[\boldsymbol{Q} - \hat{\boldsymbol{k}}(\hat{\boldsymbol{k}} \cdot \boldsymbol{Q})] \int \mathrm{d}\boldsymbol{r}\, e^{-i(\boldsymbol{k}+\boldsymbol{Q})\boldsymbol{r}} \zeta(\boldsymbol{r})$, where the factor in brackets separates the transverse component of the force and the summation over the reciprocal VL vector $\boldsymbol{Q}$ appears because the force is applied in discrete sites of the VL. Collecting contributions from all Fourier components $\boldsymbol{u}(\boldsymbol{k}) = \boldsymbol{f}(\boldsymbol{k})/C(\boldsymbol{k})$, we obtain the mean-square-root shear deformation at the surface:

$$\left\langle (\boldsymbol{\nabla} u)^2 \right\rangle = \left\langle \left(\frac{\partial u_x}{\partial y} + \frac{\partial u_y}{\partial x} \right)^2 \right\rangle = \frac{\varepsilon^2 \varphi_0^2}{4\pi^2} \int \frac{k^2\, \mathrm{d}\boldsymbol{k}}{C(k)^2} \sum_{\boldsymbol{Q}} Q^2 - \frac{(\boldsymbol{k} \cdot Q)^2}{k^2} S_\zeta(\boldsymbol{k} + \boldsymbol{Q}). \tag{6}$$

Here the integration over $\boldsymbol{k}$ is fulfilled over the VL Brillouin zone. In the following we shall approximate the surface corrugation spectrum by $S_\zeta(\boldsymbol{k}) = 2\pi\zeta^{*2} r_d^2 e^{-kr_d}$, where the corrugation correlation radius r_d is determined by the spectrum cut-off k_c, if $k_\mathrm{c}\xi < 1$: $r_d \sim k_\mathrm{c}^{-1}$. But since the vortex cannot probe corrugation on scales less than its "size" ξ, $r_d \sim \xi$ if $k_\mathrm{c}\xi > 1$. Approximating the sum over $\boldsymbol{Q}$ by an integral, we obtain for $k \sim 1/a_0 \ll Q \sim 1/r_d$

$$\left\langle (\boldsymbol{\nabla} u)^2 \right\rangle = \frac{\varepsilon^2 \varphi_0^2 a_0^2}{8\pi} \int_0^{2/a_0} \frac{k^3\, \mathrm{d}k}{C(k)^2} \int_0^\infty S_\zeta(Q) Q^3\, \mathrm{d}Q \approx \frac{\varepsilon B}{C_{66}} \frac{3r_d^2}{l_0^2}\,. \tag{7}$$

Here we used the expression $C(k) \approx k\varphi_0(C_{66}\varepsilon/B)^{1/2}$ for large k, which is a good approximation when $\lambda \gg a_0$. Note that since $C(k) \propto k$ at small k, the integral for the mean-square-root displacement $\langle \boldsymbol{u}^2 \rangle$ is divergent. This means that even a weak disorder destroys the long-range order near the surface, as was revealed in ref. [15]. However, our analysis shows that destruction of long-range order near the surface is not essential for the peak effect, which is governed by the mean-square-root deformation, but not by the mean-square-root displacement.

In the third step we derive the boundary condition eq. (2) by taking into account VL elasticity (collective pinning). In the AC experiment, the electromagnetic fields produce additional quasistatic uniform displacements $\boldsymbol{u}$ superimposed on the static random displacements induced by pinning. Because of surface disorder the uniform displacement produces a random force on vortices, which can be obtained from expansion of the random pinning force

$\boldsymbol{f}(\boldsymbol{r}_i) = -\varepsilon\varphi_0 \boldsymbol{\nabla}\zeta(\boldsymbol{r}_i + \boldsymbol{u})$ with respect to $\boldsymbol{u}$: $\delta\boldsymbol{f}_m(\boldsymbol{r}_i) = -\varepsilon\varphi_0 \boldsymbol{u}_n \partial^2\zeta(\boldsymbol{r}_i)/\partial x_m \partial x_n$. However, the uniform displacement does not produce an average force: $\langle\delta\boldsymbol{f}(\boldsymbol{r}_i)\rangle = 0$. The fluctuating force produces fluctuating displacements $\delta\boldsymbol{u}(\boldsymbol{r}_i)$, which can be found in the Fourier presentation where $\delta\boldsymbol{u}(\boldsymbol{k}) = \delta\boldsymbol{f}(\boldsymbol{k})/C(\boldsymbol{k})$. In contrast to the uniform displacement, the fluctuating displacements $\delta\boldsymbol{u}(\boldsymbol{r}_i)$ do produce an average pinning force which should be balanced by the uniform line-tension force:

$$\frac{\partial \boldsymbol{u}_m}{\partial z} + \frac{\partial^2\zeta(\boldsymbol{r}_i)}{\partial x_m \partial x_n}\,\delta\boldsymbol{u}_n(\boldsymbol{r}_i) = 0. \tag{8}$$

Since $\delta\boldsymbol{u}$ is proportional to $\boldsymbol{u}$, we arrive at the boundary condition eq. (2) imposed on the averaged, *i.e.*, uniform displacement with slippage length given by

$$\frac{1}{l_{\mathrm{S}}} \simeq \frac{\varepsilon\varphi_0}{4\pi^2} \int_{\boldsymbol{Q}} \mathrm{d}k\, |\boldsymbol{k}+\boldsymbol{Q}|^2 \left[Q^2 - \frac{(\boldsymbol{k}\cdot Q)^2}{k^2}\right] \times \frac{S_\zeta(\boldsymbol{k}+\boldsymbol{Q})}{C(k)}\,. \tag{9}$$

The same approximations as in calculating $\langle(\boldsymbol{\nabla}u)^2\rangle$ yield

$$\frac{1}{l_{\mathrm{S}}} \simeq \frac{\varepsilon\varphi_0 a_0^2}{8\pi} \int_0^{2/a_0} \frac{k\,\mathrm{d}k}{C(k)} \int_0^{\infty} S_\zeta(Q) Q^5\,\mathrm{d}Q \approx \sqrt{\frac{\varepsilon B}{C_{66}}}\,\frac{5! a_0}{2 l_0^2}\,. \tag{10}$$

Comparing with the expression $l_{\mathrm{S}} = l_0 L_c/a_0$, we see that the size of the Larkin-Ovchinnikov domain is $L_{\mathrm{c}} \sim l_0 a_0 \sqrt{C_{66}/\varepsilon\varphi_0}$. In deriving eq. (10) we have used the perturbation theory, which is valid until $L_{\mathrm{c}} \gg a_0$, or $l_{\mathrm{S}} \gg l_0$.

For low magnetic fields $B \ll B_{c2}$, one has $\varepsilon \sim (\varphi_0/\mu_0\lambda^2)\ln(B_{c2}/B)$, $C_{66} \sim \varphi_0 B/\mu_0\lambda^2$ and, according to eq. (10), $l_{\mathrm{S}} \propto \sqrt{B/\ln(B_{c2}/B)}$. Then the surface pinning length $L_{\mathrm{S}} \propto [B/\ln(B_{c2}/B)]^{3/2}$ grows with B in qualitative agreement with the experiment (fig. 3). This is the regime of collective pinning when $l_{\mathrm{S}} > l_0$. At the same time, since $r_d \ll a_0$, the vortex lattice shear deformation remains small according to eq. (7). For fields close to B_{c2}, $\varepsilon \sim (B_{c2}-B)/\mu_0\kappa^2$, $C_{66} \sim (B_{c2}-B)^2/\kappa^2$, and $r_d \sim a_0 \sim \xi$. Then eqs. (7) and (10) yield $\langle(\boldsymbol{\nabla}u)^2\rangle \approx (\xi^2/l_0^2)B_{c2}/(B_{c2}-B)$ and $l_{\mathrm{S}} \approx (l_0^2/\xi)\sqrt{(B_{c2}-B)/B_{c2}}$. Thus l_{S} decreases when B approaches B_{c2} and for $B_{c2} - B < B_{c2}\xi^2/l_0^2$ becomes smaller than l_0. This means that surface pinning ceases to be collective and the crossover to individual pinning occurs. At the same time, at $B_{c2} - B \sim B_{c2}\xi^2/l_0^2$, the deformation $\langle(\boldsymbol{\nabla}u)^2\rangle$ becomes of order unity, which means that the crystalline order at the surface is destructed even at short scales $\sim a_0$. We can call this state *surface glass*. Thus the crossover from collective to individual pinning is accompanied by the crossover from a weakly disordered crystal to a glass state at the surface.

Still, this crossover cannot explain a fully developed PE. Despite $l_{\mathrm{S}} \propto \sqrt{B_{c2}-B}$ decreases at B approaching B_{c2}, according to eq. (1), $1/L_{\mathrm{S}}$ continues to decrease proportionally to $\sqrt{B_{c2}-B}$, whereas in the experiment (fig. 3) $1/L_{\mathrm{S}}(B)$ increases on the left of the peak. Nevertheless, the growth of the deformation $\langle(\boldsymbol{\nabla}u)^2\rangle$, which accompanies the decrease of l_{S}, eventually invalidates the linear elasticity theory used above. Qualitatively this can be corrected by introducing the renormalized deformation-dependent shear modulus: $\tilde{C}_{66} = C_{66}(1 - \alpha\langle(\boldsymbol{\nabla}u)^2\rangle) \approx C_{66}(1 - B/B_{\mathrm{pk}})$. Here the field B_{pk} corresponds to the crystal-glass transition, where $\tilde{C}_{66} = 0$, and α is an unknown numerical factor, which could be close to 0.1 as in the Lindemann criterion. Using renormalized modulus $\tilde{C}_{66}$ in place of C_{66} in eq. (10) we obtain that l_{S} (as well as L_{S}, see eq. (1)) decreases proportionally to $1/\sqrt{B_{\mathrm{pk}}-B}$ in qualitative agreement with experiment (fig. 3). On the right of the peak, pinning is individual and $l_{\mathrm{S}} \sim l_0$ does not depend on B, while $1/L_{\mathrm{S}} \propto (B_{c2}-B)$ decreases with B. We should stress, however, that our "surface-disorder" scenario is relevant only for a close vicinity

of the peak effect. At further approach of the magnetic field to the upper critical field B_{c2} disorder should expand from the surface to the bulk where in principle it can compete with the transition to the liquid state. Therefore our results do not contradict observations of the bulk vortex-liquid state above the peak effect in ref. [14].

The close relation between PE and vanishing of the shear modulus of VL was suggested in the early studies of PE [3, 4]. The new feature of our scenario is that at $B < B_{pk}$ the shear modulus vanishes only at distances on the order of the deformation penetration depth $1/p \propto 1/\sqrt{\tilde{C}_{66}}$ from the surface. Our scenario agrees with STM imaging of the vortex array by Troyanovski *et al.* [16]. They revealed that PE is accompanied by the disorder onset on *the surface* of a 2H-$NbSe_2$ sample, but they related it with bulk pinning. In order to discriminate two scenarios, it would be useful to supplement the STM probing of the vortex array at the surface by probing vortex arrangements in the bulk.

In conclusion, we presented the experiment and the theory, which support a new scenario for the peak effect based on competition between vortex-lattice shear rigidity and weak surface disorder. The peak is accompanied by a crossover from collective to individual vortex pinning and from a weakly disordered crystal to a glass state at the sample surface. Beside its experimental relevance, this mechanism offers an interesting paradigm for elastic systems at the upper critical dimension for disorder.

* * *

We thank F. R. Ladan and E. Lacaze for the ion-beam etching and AFM measurements. We acknowledge discussions with B. Horowitz, T. Natterman and T. Giamarchi. This work was funded by the French-Israel program Keshet and by the Israel Academy of Sciences and Humanities. The Laboratoire Pierre Aigrain is "unité mixte de recherche" (UMR8551) of the Ecole Normale, the CNRS, and the universities Paris 6 and Paris 7.

REFERENCES

[1] Autler S. H., Rosenblum E. S. and Gooen K. H., *Phys. Rev. Lett.*, **9** (1962) 489.
[2] Kes P. H. and Tsuei C. C., *Phys. Rev. Lett.*, **47** (1981) 1930.
[3] Pippard A. B., *Philos. Mag.*, **19** (1969) 217.
[4] Larkin A. I. and Ovchinnikov Y. N., *J. Low Temp. Phys.*, **34** (1979) 409.
[5] Lütke-Entrup N., Plaçais B., Mathieu P. and Simon Y., *Phys. Rev. Lett.*, **79** (1997) 2538.
[6] Lütke-Entrup N., Plaçais B., Mathieu P. and Simon Y., *Physica B*, **255** (1998) 75.
[7] Campbell A. M., *J. Phys. C*, **2** (1969) 1492.
[8] Coffey M. and Clem J., *Phys. Rev. B*, **45** (1992) 9872.
[9] Sonin E. B., Tagantsev A. K. and Traito K. B., *Phys. Rev. B*, **46** (1992) 5830.
[10] Williamson S. J., *Phys. Rev. B*, **2** (1970) 3545.
[11] Abrikosov A. A., *Sov. Phys. JETP*, **5** (1957) 1174.
[12] Krusius M., Korhonen J. S., Kondo Y. and Sonin E. B., *Phys. Rev. B*, **47** (1993) 15113.
[13] Paltiel Y., Zeldov E., Myasoedov Y., Rappaport M. L., Jung G., Bhattacharya S., Higgins M. J., Xiao Z. L., Andrei E. Y., Gammel P. L. and Bishop D. J., *Phys. Rev. Lett.*, **85** (2000) 3712.
[14] Ling X. S., Park S. R., McClain B. A., Choi S. M., Dender D. C. and Lynn J. W., *Phys. Rev. Lett.*, **86** (2001) 712.
[15] Feldman D. E. and Vinokur V. M., *Phys. Rev. Lett.*, **89** (2002) 227204.
[16] Troyanovski A. M., van Hecke M., Saha N., Aarts J. and Kes P. H., *Phys. Rev. Lett.*, **89** (2002) 147006.